PRAMANA
— journal of
physics

Vol. 61, No. 3
September 2003
pp. 563–575

Phase conjugation of gap solitons: A numerical study

V S C MANGA RAO and S DUTTA GUPTA*
School of Physics, University of Hyderabad, Hyderabad 500 046, India
*Corresponding author
Email: sdgsp@uohyd.ernet.in

MS received 2 January 2003; revised 28 June 2003; accepted 3 July 2003

Abstract. We study the effect of a nearby phase-conjugate mirror (PCM) on the gap soliton of a Kerr non-linear periodic structure. We show that phase conjugation of the gap soliton (in the sense of replication of the amplitude profile in the reverse direction) is possible under the condition of PCM reflectivity approaching unity. This is in contrast with the results for linear structures, where the wave profiles can be conjugated for arbitrary values of the PCM reflectivity. The sensitivity of the conjugation of the gap solitons to PCM reflectivity is ascribed to the fine balance of non-linearity with dispersion, necessary for their existence.

Keywords. Phase conjugation; non-linear optical waveguides; optical solitons; optical bistability.

PACS Nos 42.65.Hw; 42.65.Tg; 42.65.Wi; 42.65.Pc

1. Introduction

In the past two decades, there has been considerable interest in non-linear periodic structures [1–10]. It is well-known that linear periodic structures possess pass and stop gaps, which can be manipulated by addition of non-linearity. This led to a diversity of applications of non-linear periodic structures like optical limiting, all optical switching etc [1,2]. One of the major discoveries in this context was that of gap solitons (also referred to as Bragg solitons) in Kerr non-linear periodic structures [3–5], which were first reported by Chen *et al* [3]. They are characterized by a sech field distribution corresponding to the total transmission states of the non-linear structure. The frequency of the wave is close to one of the edges inside the gap (of the linear structure). Thus non-linearity induced deformation and the shift renders the otherwise opaque system transparent. The typical gap soliton emerges when the system is totally transparent. Though there have been several indirect experimental evidences of gap solitons in periodic structures [6], the first direct observation was reported by Eggleton *et al* [7]. Since then there have been experimental studies reporting gap soliton-induced all-optical switching with large contrast [8]. All optical logic operations using coupled gap solitons have also been reported [9]. Very recently, a new class of Raman gap solitons [10] has been proposed, where the pump pulse is far detuned from the Bragg resonance. These Raman gap solitons are shown to be robust,

surviving even after the passage of the pump pulse. All these studies clearly demonstrate the potential of gap solitons for all-optical information processing and other critical non-linear optical applications.

Another interesting area which has attracted considerable attention in the past decade is linear or non-linear layered media near a phase-conjugate mirror (PCM) [11–13]. It was shown that the presence of the PCM can lead to significant backscattering [11,12], which is due to the conjugation of the modes of the layered structure. Other interesting aspects like optical bistability and multistability were demonstrated [12]. Theoretical issues like the validity of the distortion correction theorem [14] for linear as well as non-linear structures were also discussed. Later a rigorous numerical scheme for layered media near a PCM was presented by Laine *et al* [13].

Keeping in view the aforesaid, an interesting problem can be posed in the context of a non-linear periodic medium near a PCM. Since the periodic structure can lead to the formation of gap solitons, pertinent questions that can be addressed, are as follows: Can the gap soliton be phase-conjugated? If yes, under which conditions? Strictly speaking, phase conjugation of an arbitrary wave with wave vector k implies complex conjugation of spatial profile leading to a reversal of sign in k. Thus in order to check whether a given complex wave profile is phase-conjugated or not, one needs to examine both the amplitude as well as the phase of the wave. Retention of the amplitude profile (possibly with scaling) with a sign reversal in the phase will give the phase-conjugated wave. One should also note that for general finite non-linear structures it is extremely difficult to obtain the analytical solutions for the wave envelope and one needs to resort to numerical methods. In this paper we carry out an extensive numerical study of the wave profiles in both the forward and the reverse directions (along the layers). Note that forward (backward) directions are determined by the surface component of the wave vector for oblique incidence of the input plane wave. Our studies encompass both linear and non-linear structures and a comparison of the relevant features. Keeping in view the limitations of the numerical study to verify the rigorous identity of the phase and amplitude functions, we resort to a qualitative comparison of the amplitude profiles in the forward and reverse directions. We shall assert a wave to be phase-conjugated if both the forward and the reverse (phase-conjugated) waves have 'similar' intensity profiles. We will show that only under stringent conditions, i.e. only for the phase-conjugate reflectivity approaching the value unity, such phase conjugation of the gap soliton is possible. By means of a comparison with the linear counterpart, we will show that phase conjugation of spatial profiles of the linear structures is possible for arbitrary values of the phase-conjugate reflectivity. We then present an explanation for the fact: why the condition for phase-conjugation of gap solitons is so stringent for the non-linear structure? We ascribe it to the 'fine' balance of non-linearity with dispersion of the layered media, where the PCM reflectivity plays a crucial role in determining the power level of the reflected waves. The results of our investigation can be used in soliton-based non-linear switching and other planar optical information processing devices.

The organization of the paper is as follows: In §2 we present the physical system and the mathematical model. It is a generalization of the earlier model proposed by Jose *et al* [12]. In §3, we present the numerical results pertaining to the specular and phase-conjugated reflectivities. We also present the field distribution in the layers. Finally in §4 we summarize the major findings.

2. Mathematical formulation

Here, we generalize the calculations of Jose *et al* [12] to an arbitrary non-linear layered medium in the near vicinity of a PCM. Consider the layered structure near a PCM with reflectivity μ shown in figure 1. It comprises of M layers, where any jth layer with width d_j and dielectric function ε_j can, in principle, be linear or non-linear. Let the structure be illuminated by a s-polarized plane monochromatic wave incident at angle θ. We further assume that the non-linearity in the layers are given by the induction vector

$$\vec{D}_{\mathrm{NL}} = \varepsilon\chi(A(\vec{E}\cdot\vec{E}^{*})\vec{E} + B(\vec{E}\cdot\vec{E})\vec{E}^{*}), \tag{1}$$

where A and B are Kerr and electrostriction coefficient, respectively; χ is a constant of non-linear interaction, ε the linear dielectric constant and $\vec{E}$ the local electric field. Due to the presence of PCM one would have the waves propagating in both $+y$ and $-y$ directions accompanied by multiple reflections at the interfaces. Hereafter, we will refer to $+y$ $(-y)$ direction as forward (phase-conjugated or backward). Assuming that a given jth layer $(z_{j-1} \le z \le z_j)$ is non-linear the solution for the electric field in the same can be written as

$$\vec{E}_j = \vec{E}_j^{\mathrm{f}} \mathrm{e}^{ik_y y} + \vec{E}_j^{\mathrm{b}} \mathrm{e}^{-ik_y y}, \tag{2}$$

with

$$\vec{E}_j^{\mathrm{f}} = \left(A_{j+}^{\mathrm{f}} \mathrm{e}^{-ik_{zj+}^{\mathrm{f}}(z-z_{j-1})} + A_{j-}^{\mathrm{f}} \mathrm{e}^{ik_{zj-}^{\mathrm{f}}(z-z_{j-1})}\right)\hat{e}_x, \tag{3}$$

$$\vec{E}_j^{\mathrm{b}} = \left(A_{j+}^{\mathrm{b}} \mathrm{e}^{ik_{zj+}^{\mathrm{b}}(z-z_{j-1})} + A_{j-}^{\mathrm{b}} \mathrm{e}^{-ik_{zj-}^{\mathrm{b}}(z-z_{j-1})}\right)\hat{e}_x, \tag{4}$$

where $A_{j\pm}^{\mathrm{f}}(A_{j\pm}^{\mathrm{b}})$ are amplitudes of the forward (phase-conjugated) waves, z_{j-1} is the distance of jth layer from PCM. Note that eqs (3) and (4) hold under slowly varying envelope

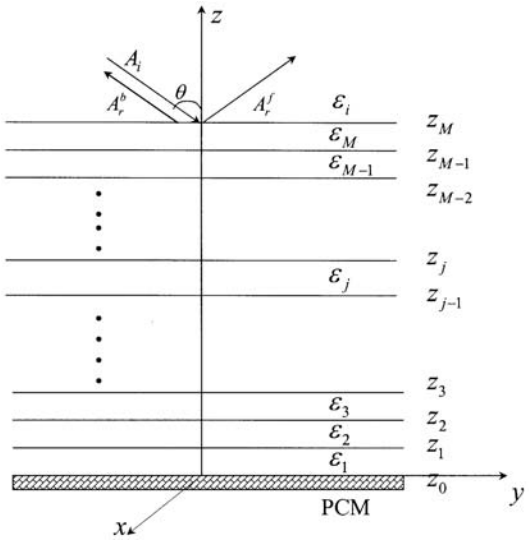

Figure 1. Schematic view of the layered medium near a PCM.

approximation (SVEA). These complex amplitudes in turn define the z-component of the wave vector as follows:

$$k^{\mathrm{f}}_{zj\pm} = k_0 p_j \left(1 + \frac{\alpha_j}{p_j^2}\left(|A^{\mathrm{f}}_{j\pm}|^2 + 2|A^{\mathrm{f}}_{j\mp}|^2\right)\right)^{1/2}, \tag{5}$$

$$k^{\mathrm{b}}_{zj\pm} = k_0 p_j \left(1 + \frac{\alpha_j}{p_j^2}\left(|A^{\mathrm{b}}_{j\pm}|^2 + 2|A^{\mathrm{b}}_{j\mp}|^2\right)\right)^{1/2}, \tag{6}$$

where

$$p_j = \left(\varepsilon_j - (k_y/k_0)^2\right)^{1/2}, \tag{7}$$

$$\alpha_j = \chi(A+B)\varepsilon_j, \tag{8}$$

$$k_y = k_0\sqrt{\varepsilon_i}\sin\theta_i, \quad k_0 = \frac{\omega}{c}. \tag{9}$$

p_j is the normalized z-component of the wave vector, k_y the surface component of the wave vector determined by the angle of incidence. In writing eqs (3) and (4) we have used the approximation of lossless medium ($\mathrm{Im}(\varepsilon_j) = 0$) and weak non-linearity (i.e. $\alpha \ll 1$). The corresponding magnetic field in the jth layer can be derived from eq. (2) and the Maxwell equations. Results for a linear layer can be easily recovered from eqs (2)–(7) by setting $\alpha = 0$ leading to $k^{\mathrm{f}}_{zj\pm} = k^{\mathrm{b}}_{zj\pm} = k_{zj} = k_0 p_j$.

For incidence of s-polarized plane wave the electric field in the medium of incidence can be written as

$$\vec{E}_i = \left[\left(A_{\mathrm{i}}\mathrm{e}^{-ik_{zi}(z-z_M)} + A^{\mathrm{f}}_{\mathrm{r}}\mathrm{e}^{ik_{zi}(z-z_M)}\right)\mathrm{e}^{ik_y y} + \left(A^{\mathrm{b}}_{\mathrm{r}}\mathrm{e}^{ik_{zi}(z-z_M)}\right)\mathrm{e}^{-ik_y y}\right]\hat{e}_x. \tag{10}$$

Here A_{i}, $A^{\mathrm{f}}_{\mathrm{r}}$ and $A^{\mathrm{b}}_{\mathrm{r}}$, are the complex amplitudes of the incident, reflected and backscattered (phase-conjugated) amplitudes, respectively. The quantities of interest are specular or forward and phase-conjugated reflectivities, R_{f} and R_{b}, respectively, defined as follows:

$$R_{\mathrm{f}} = \left|\frac{A^{\mathrm{f}}_{\mathrm{r}}}{A_{\mathrm{i}}}\right|^2, \quad R_{\mathrm{b}} = \left|\frac{A^{\mathrm{b}}_{\mathrm{r}}}{A_{\mathrm{i}}}\right|^2. \tag{11}$$

The unknown amplitudes $A^{\mathrm{f}}_{\mathrm{r}}$, $A^{\mathrm{b}}_{\mathrm{r}}$ and $A^{\mathrm{f}}_{j\pm}$, $A^{\mathrm{b}}_{j\pm}$ are to be determined from the boundary conditions of the continuity of the tangential component of the electric and magnetic fields at the interfaces. We also need the boundary conditions at the PCM interface (i.e. $z = 0$), which can be written as

$$A^{\mathrm{b}}_{1+} = \mu\,(A^{\mathrm{f}}_{1+})^*, \quad A^{\mathrm{f}}_{1-} = \mu\,(A^{\mathrm{b}}_{1-})^*. \tag{12}$$

It is clear from eqs (2)–(4) and (12) that there is no direct coupling between the forward and phase-conjugated waves in any of the non-linear layers, except at the PCM interface. Since some of the layers are non-linear and multistability is expected, we proceed in a reverse order and treat $A^{\mathrm{b}}_{\mathrm{r}}$ as the parameter, propagate this wave down the structure to the PCM. Thus we evaluate the complex amplitudes for the phase conjugated waves in all the layers. Use of eq. (12) leads to the forward wave amplitudes at the PCM interface. Back

propagating this wave up the structure into the incident medium leads to complex amplitudes for the forward wave in all the layers. The remaining part of this section illustrates the steps involved, which can be reduced to matrix equations involving the relevant transfer matrices.

Henceforth, we introduce dimensionless fields as $\bar{A}_j = \left(\sqrt{\alpha}/p_j\right) A_j$. The dimensionless amplitudes in any jth layer can be expressed in terms of $\bar{A}^{\mathrm{b}}_{\mathrm{r}}$ as follows:

$$\begin{pmatrix} \bar{A}^{\mathrm{b}}_{j+} \\ \bar{A}^{\mathrm{b}}_{j-} \end{pmatrix} = (M^{\mathrm{b}}_j)^{-1} P^{\mathrm{b}}_{j-1} (M^{\mathrm{b}}_{j-1})^{-1} \cdots (M^{\mathrm{b}}_{M-1})^{-1} P^{\mathrm{b}}_M (M^{\mathrm{b}}_M)^{-1} \begin{pmatrix} 1 \\ p_i \end{pmatrix} \bar{A}^{\mathrm{b}}_{\mathrm{r}}. \quad (13)$$

Introducing dimensionless intensities $U^{\mathrm{b}}_{j\pm}$ as $U^{\mathrm{b}}_{j\pm} = |\bar{A}^{\mathrm{b}}_{j\pm}|^2$, eq. (13) reduces to

$$\begin{pmatrix} U^{\mathrm{b}}_{j+} \\ U^{\mathrm{b}}_{j-} \end{pmatrix} = \left| (M^{\mathrm{b}}_j)^{-1} P^{\mathrm{b}}_{j-1} (M^{\mathrm{b}}_{j-1})^{-1} \cdots (M^{\mathrm{b}}_{M-1})^{-1} P^{\mathrm{b}}_M (M^{\mathrm{b}}_M)^{-1} \begin{pmatrix} 1 \\ p_i \end{pmatrix} \right|^2 U^{\mathrm{b}}_{\mathrm{r}}, \quad (14)$$

where M and P are 2×2 matrices. For example, for any jth layer we have

$$M^{\mathrm{b}}_j = \begin{pmatrix} \mathrm{e}^{ip^{\mathrm{b}}_{j+}\bar{d_j}} & \mathrm{e}^{-ip^{\mathrm{b}}_{j-}\bar{d_j}} \\ p^{\mathrm{b}}_{j+}\mathrm{e}^{ip^{\mathrm{b}}_{j+}\bar{d_j}} & -p^{\mathrm{b}}_{j-}\mathrm{e}^{-ip^{\mathrm{b}}_{j-}\bar{d_j}} \end{pmatrix}, \quad (15)$$

$$P^{\mathrm{b}}_j = \begin{pmatrix} 1 & 1 \\ p^{\mathrm{b}}_{j+} & -p^{\mathrm{b}}_{j-} \end{pmatrix}. \quad (16)$$

In eq. (14), $||^2$ implies the square of the modulus of the elements of the column matrix in the right-hand side and the dimensionless thickness $\bar{d_j}$ and the wave number $p^{\mathrm{b}}_{j\pm}$ are respectively, given by

$$\bar{d_j} = k_0(z_j - z_{j-1}), \quad p^{\mathrm{b}}_{j\pm} = p_j(1 + U^{\mathrm{b}}_{j\pm} + 2U^{\mathrm{b}}_{j\mathrm{m}})^{1/2}. \quad (17)$$

Note that if any layer happens to be non-linear then eq. (14) for the intensities $U^{\mathrm{b}}_{j\pm}$ represent a set of two coupled non-linear transcendental equations, since the matrix M^{b}_j on the right-hand side contains the intensity-dependent wave vectors involving the unknowns themselves. On the other hand, if the layer is linear then the propagation through it is given by the standard characteristic matrix [15] which can be obtained from eq. (15) by replacing $p^{\mathrm{b}}_{j\pm}$ by p_j.

A knowledge of the phase-conjugated intensities in layer '1' and use of the boundary conditions (eq. (12)) immediately leads to the forward wave intensities

$$\begin{pmatrix} U^{\mathrm{f}}_{1+} \\ U^{\mathrm{f}}_{1-} \end{pmatrix} = \begin{pmatrix} \frac{1}{|\mu|^2} & 0 \\ 0 & |\mu|^2 \end{pmatrix} \begin{pmatrix} U^{\mathrm{b}}_{1+} \\ U^{\mathrm{b}}_{1-} \end{pmatrix}. \quad (18)$$

Analogous to eq. (14), the matrix equations for the forward wave intensities in any kth layer, $U^{\mathrm{f}}_{k\pm}$ can be written as

$$\begin{pmatrix} U^{\rm f}_{k+} \\ U^{\rm f}_{k-} \end{pmatrix} = \left| (P^{\rm f}_k)^{-1} M^{\rm f}_{k-1} (P^{\rm f}_{k-1})^{-1} \cdots (P^{\rm f}_3)^{-1} M^{\rm f}_2 (P^{\rm f}_2)^{-1} M^{\rm f}_1 \begin{pmatrix} \bar{A}^{\rm f}_{1+} \\ \bar{A}^{\rm f}_{1-} \end{pmatrix} \right|^2, \qquad (19)$$

Here the matrices $M^{\rm f}$ and $P^{\rm f}$ are given by eqs (15) and (16) with the following modifications:

$$M^{\rm f}_j = M^{\rm b}_j (p^{\rm b}_{j\pm} \to p^{\rm f}_{j\pm}, \bar{d_j} \to -\bar{d_j}), \qquad (20)$$

$$P^{\rm f}_j = P^{\rm b}_j (p^{\rm b}_{j\pm} \to p^{\rm f}_{j\pm}), \qquad (21)$$

with

$$p^{\rm f}_{j\pm} = p_j (1 + U^{\rm f}_{j\pm} + 2U^{\rm f}_{j{\rm m}})^{1/2}. \qquad (22)$$

The incident and reflected intensities in the medium of incidence are then given by

$$\begin{pmatrix} U_{\rm i} \\ U^{\rm f}_{\rm r} \end{pmatrix} = \left| (P_1)^{-1} M^{\rm f}_M \begin{pmatrix} \bar{A}^{\rm f}_{M+} \\ \bar{A}^{\rm f}_{M-} \end{pmatrix} \right|^2. \qquad (23)$$

The knowledge of given $U^{\rm b}_{\rm r}$ and eq. (23) straight away leads to the phase conjugate and specular reflectivities $R_{\rm b}$ and $R_{\rm f}$, respectively.

3. Numerical results

We apply the procedure developed in the previous section to a non-linear superlattice near a PCM. The structure consists of 26 periods of alternating linear and non-linear layers with dielectric constants ε_b (with width d_b) and ε_a (with width d_a), respectively. The a-type layers (except for the layer adjacent to the PCM) are assumed to be non-linear with third-order non-linearity given by eq. (1). The layered structure is loaded on top by a linear medium with dielectric constant ε_i. Analogous structure [16] without the PCM was earlier considered to show the existence of gap solitons by means of plotting the sum intensity $U_j = U_{j+} + U_{j-}$ against the layer number j [17]. As discussed earlier, gap solitons in this system emerge as the total transmission states of the non-linear structure. In this paper, we present a somewhat better description by looking at the actual intensity profiles of the waves. Moreover, we study the effect of the PCM on such excitations. For all our numerical calculations, we have chosen the following system parameters: $\varepsilon_i = 12.25$, $\varepsilon_a = 12.25$, $\varepsilon_b = 10.24$, $d_a = 0.54\lambda$, $d_b = 0.2\lambda$ (λ – wavelength). Calculations have been carried out for two values of the PCM reflectivities, namely, $\mu = 0.01$ and $\mu = 0.99$. Choosing one of the values of μ close to unity is for checking the consequences of the distortion correction theorem [14], i.e., the well-known ability of such PCMs to correct for distortions in the absence of losses and evanescent waves. We start by looking at the linear properties of the structure which are shown in figure 2. The top (bottom) row in figure 2 displays the results for the specular (phase-conjugated) reflectivity $R_{\rm f}$ ($R_{\rm b}$). The left (right) panel gives the results for $\mu = 0.99$ ($\mu = 0.01$). It is clear from figure 2 that there are sharp resonance dips in the reflectivity for smaller values of the PCM reflectivity. For future reference we label the resonance dips in figure 2 (top row) from right to left. Thus the first resonance occurs at $\theta = 80.5755^\circ$, the second at $\theta = 80.556^\circ$, etc. In the absence of the PCM, these dips would have corresponded to sharp transmission resonances [16], which is due to

tunneling through the lower index *b*-type layers. Note that for the chosen range of angles ($\theta > \theta_{\rm TIR} = 66.1^\circ$) waves are evanescent in *b*-type layers. The presence of the PCM leads to phase-conjugate reflectivity, which mimics the transmission resonances though with scaled down features due to low $\mu = 0.01$ (note the vertical scale in the right bottom curve). As the PCM reflectivity is increased to $\mu = 0.99$ the central resonance features in $R_{\rm f}$ are suppressed, leading to almost close to unity resonance peaks in $R_{\rm b}$. In fact, for μ approaching unity one ends up with a $R_{\rm f} \sim 0$ and $R_{\rm b} \sim 1$ band between $78.4^\circ < \theta < 80.58^\circ$ (not shown). This unusual result can be understood in the light of the distortion correction theorem. Note that the distortion correction theorem is *not* applicable in a rigorous sense, since the waves are evanescent in *b*-type layers. However, due to small thickness of the *b*-type layers and almost complete tunneling to the subsequent layers, the role of evanescent waves is minimized and one can still apply the distortion correction theorem. The wave that is incident on the structure will be phase-conjugated leading to $R_{\rm f} \sim 0$ and $R_{\rm b} \sim 1$. This curious interference effect is obviously due to the exotic properties of the PCM. One has an 'almost perfect' band out of a finite periodic structure. Recall that perfect bands result only in infinite periodic structure.

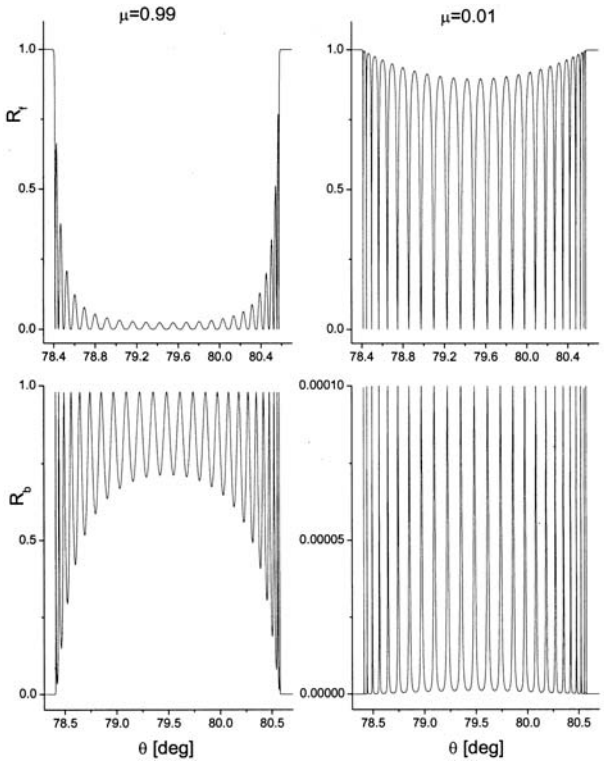

Figure 2. Linear response of the periodic structure near a PCM. Top (bottom) curve shows the forward (phase-conjugated) reflectivity $R_{\rm f}(R_{\rm b})$ as functions of the angle of incidence θ for two values of the PCM reflectivity μ, namely $\mu = 0.99$ (left curves) and $\mu = 0.01$ (right curves). Other system parameters are as follows: $\varepsilon_i = 12.25,\ \varepsilon_a = 12.25,\ \varepsilon_b = 10.24,\ d_a = 0.55\lambda,\ d_b = 0.2\lambda$.

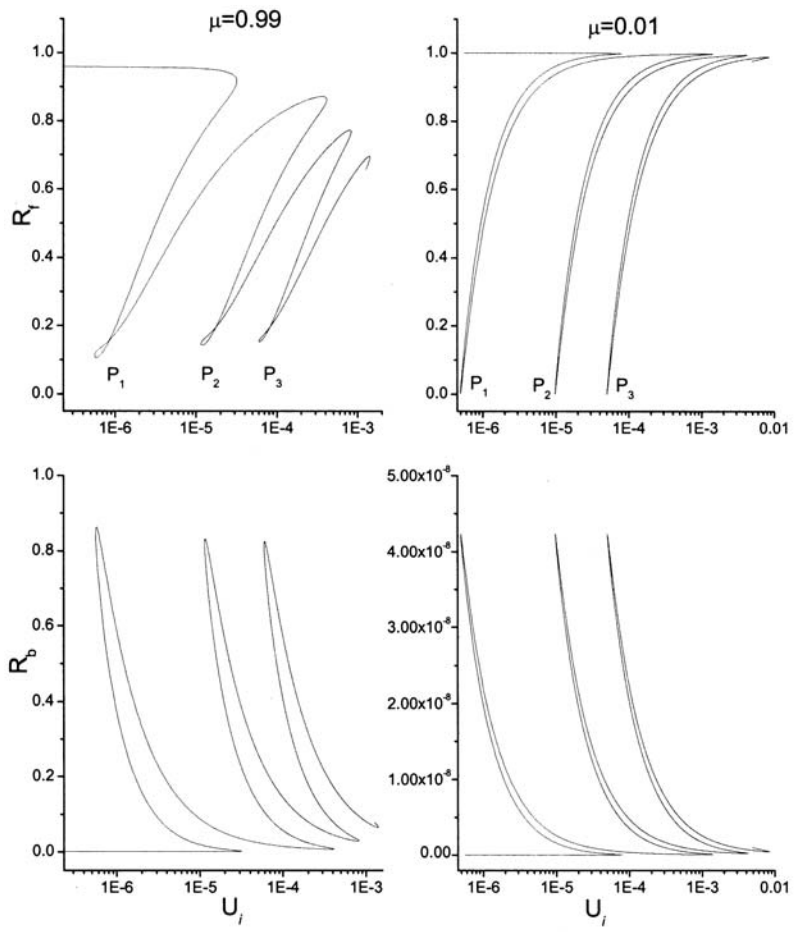

Figure 3. Forward (top row) and phase-conjugated (bottom row) reflectivities R_f and R_b, respectively, for the non-linear periodic structure near a PCM at $\theta = 80.58°$ for $\mu = 0.99$ (left curves) and $\mu = 0.01$ (right curves). Other parameters are as in figure 2.

We now present the results for the non-linear structures. As mentioned earlier we treat U_r^b $(= |\overline{A}_\mathrm{r}^\mathrm{b}|^2)$ as the parameter and look at the input–output characteristics. The angle θ is chosen in the 'rejection' band ($R_\mathrm{f} \sim 1$) of the corresponding linear structure. An increase in the input intensity leads to a relative shift of the 'allowed' band ($R_\mathrm{f} \sim 0$) to the right. The results for the non-linear reflection dips in R_f (top row) and corresponding transmission peaks in R_b (bottom row) are shown in figure 3. Again the left (right) panel gives the results for $\mu = 0.99$ ($\mu = 0.01$). These resonance dips in figure 3 are also labeled sequentially by P_1, P_2, ... One thus has the usual multistability for non-linear layered media. Note also that for larger value of μ (e.g. $\mu = 0.99$) one has the formation of loops in R_f, which is reminiscent of the isolas reported earlier [18].

At this stage it would be proper to point out the differences between the present structure and the one studied earlier by Jose *et al* [12]. Jose *et al* studied the effect of the PCM on the

modes of a non-linear waveguide. Since the fields were evanescent in the layer adjacent to PCM, the thickness of that layer played a key role in controlling the coupling of the guided wave with the PCM. In contrast, we now have propagating waves in the layer bounding the PCM. Thus the thickness of this layer plays an insignificant role of adding a phase without affecting the amplitudes.

Since the primary goal is to probe the feasibility of phase conjugation of the wave profiles, one needs to look at the field distribution corresponding to the forward and backward waves for various linear and non-linear resonant states. The intensity distribution when the first linear resonant state is excited at $\theta = 80.5755^\circ$, is shown in figure 4. We have shown the normalized forward and backward intensities V_f and V_b, respectively, as a function of z (in units of λ) in figure 4. For example, V_f is defined as

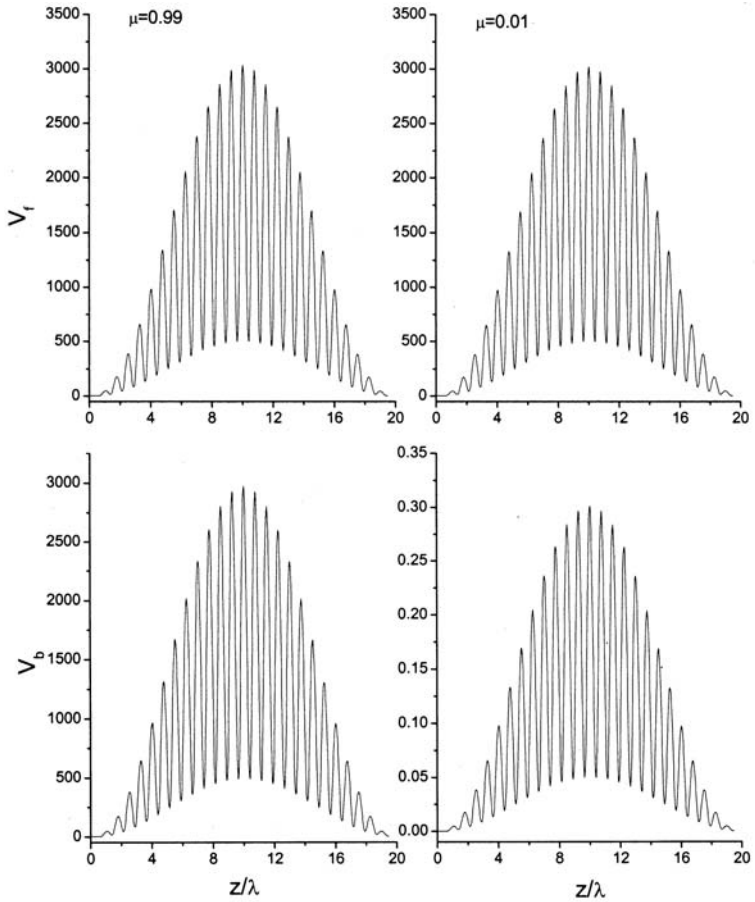

Figure 4. Normalized intensity distributions corresponding to the first linear resonance at $\theta = 80.5755^\circ$ of the forward and the phase-conjugated waves, V_f (top row) and V_b (bottom row), respectively, for $\mu = 0.99$ (left) and $\mu = 0.01$ (right). Other parameters are as in figure 2.

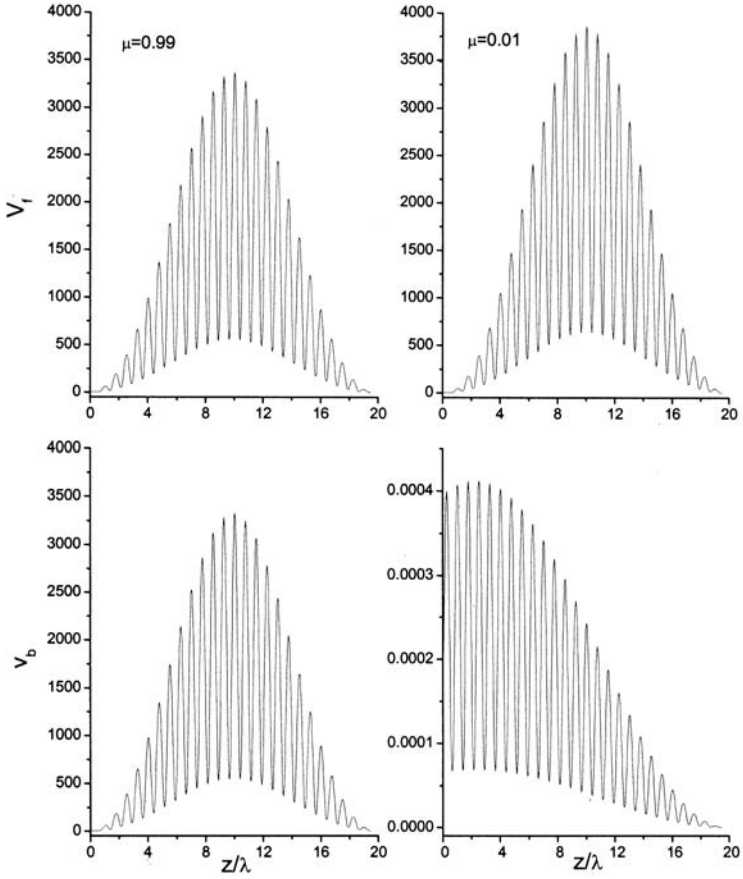

Figure 5. Normalized intensity distributions for the forward (top row) and phase-conjugated (bottom row) waves corresponding to the first non-linear resonance (points P_1 of figure 3) for $\theta = 80.58°$. The left (right) curves are for $\mu = 0.99$ ($\mu = 0.01$) and the corresponding parameters are: $U_r^b = 4.7431 \times 10^{-7}$, $U_i = 5.60157 \times 10^{-6}$ ($U_r^b = 2.1037 \times 10^{-14}$, $U_i = 4.9651 \times 10^{-7}$). Other parameters are as in figure 2.

$$V_f = \frac{\alpha}{p^2}|E^f|^2/U_i. \tag{24}$$

The top (bottom) row in figure 4 corresponds to forward (phase conjugate) wave of the structure and the left (right) panel corresponds to the PCM reflectivity $\mu = 0.99$ ($\mu = 0.01$). It is clear from a comparison of the top and bottom rows in figure 4, that for the linear structure the field profiles of the forward waves can be replicated in the backward direction for all values of μ.

The scenario is quite different for the non-linear system. In figure 5, we show the profiles, when the first non-linear resonant state is excited. The left panel shows the intensity distribution for $\mu = 0.99$ corresponding to point P_1 of the top left panel of figure 3. Other parameters are $\theta = 80.58°, U_r^b = 4.7431 \times 10^{-7}$, which corresponds to an input intensity

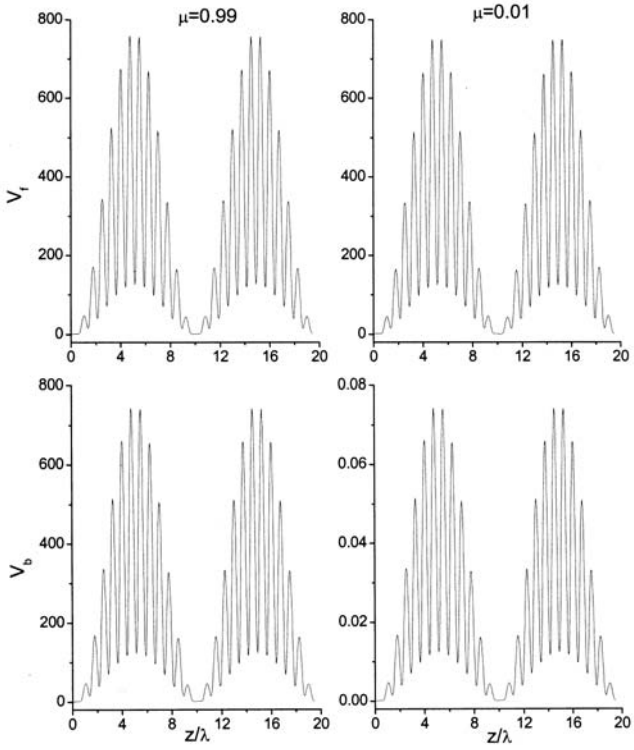

Figure 6. Same as in figure 4, except for the second linear resonance at $\theta = 80.556°$.

$U_i = 5.60157 \times 10^{-6}$. The right panel gives the same for $\mu = 0.01, U_r^b = 2.1037 \times 10^{-14}$, with an input intensity $U_i = 4.9651 \times 10^{-7}$. It is clear from figure 5 that the forward wave profile can be replicated in the reverse direction for $\mu = 0.99$ while for $\mu = 0.01$ one ends up with a completely different intensity distribution in the backward direction. Thus gap solitons can be phase-conjugated only for μ approaching the value unity, i.e. when the conditions for the distortion correction theorem are met. Here again we are referring to the distortion correction theorem with the allowance for evanescent waves in thin *b*-type layers with almost complete tunneling. This result is not difficult to understand if one recalls that the existence of gap solitons in the non-linear periodic structure hinges on a delicate balance of dispersion and non-linearity. The phase-conjugated wave should have sufficient power level to maintain this delicate balance in order to be the replica of the forward gap soliton. This is possible only under the condition that $\mu \sim 1$. Deviating from this value would result in disturbing this fine balance, leading to a completely different wave profile in the backward direction (see bottom right curve in figure 5).

The above results for the single hump distribution (for linear) and gap solitons (for the non-linear structure) can be generalized to multiple hump and *N*-soliton solutions. The results for the double hump distribution for the linear structure and their phase conjugation is shown in figure 6. These intensity distributions correspond to the second linear resonance at $\theta = 80.556°$ in figure 2. From figure 6 one can easily see that the phase conjugation of

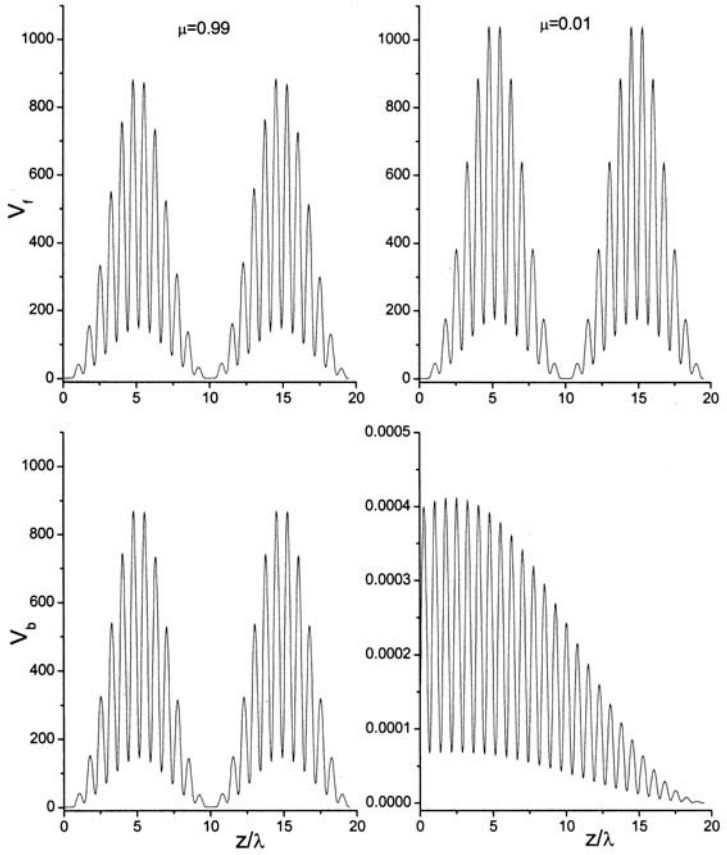

Figure 7. Same as in figure 5, except for the second non-linear resonance at $\theta = 80.58°$ (points P_2 in figure 3). The left (right) curves correspond to $\mu = 0.99$, $U_r^b = 9.6814 \times 10^{-6}$, $U_i = 1.7829 \times 10^{-4}$ ($\mu = 0.01, U_r^b = 4.129 \times 10^{-13}$, $U_i = 9.749 \times 10^{-5}$).

the profiles is independent of the value of PCM reflectivity μ. The results for the non-linear counterpart are shown in figure 7. Same conclusion as in the case of the gap soliton with one peak can be drawn. The two-peak solitons can be phase conjugated for $\mu = 0.99$, while the distinct two peaks are washed in the backward direction for $\mu = 0.01$.

4. Conclusion

In conclusion, we have carried out a detailed numerical study of a Kerr non-linear periodic medium near a phase conjugate mirror. We have investigated the feasibility of phase conjugation of the wave profiles by the PCM for both linear and non-linear structures. We have shown that irrespective of the value of the PCM reflectivity, in a linear structure it is possible to have phase conjugation of the mode profiles. In contrast, the gap solitons

of the non-linear structure can be phase-conjugated only for PCM reflectivity approaching the value unity. This has been explained by the role of the PCM reflectivity to control the fine balance of non-linearity with dispersion which is necessary for the existence of the gap solitons. This striking result, namely, distortion correction even in presence of evanescent waves holds under the conditions of resonant tunneling. However, for thick layers with evanescent waves, the tunneling is incomplete, leading to distorted phase-conjugated profile. It remains to be seen how the widths of the layers (where the waves are evanescent) affect the phase-conjugation process. Research in this direction is underway and will be reported elsewhere.

Acknowledgements

One of the authors (SDG) would like to thank the Department of Science and Technology, Government of India for financial support. MR would like to acknowledge a fellowship from Council of Scientific and Industrial Research, Government of India.

References

[1] H G Winful and G I Stegeman, *Proc. SPIE* **517**, 214 (1984)
[2] S Dutta Gupta, in *Progress in optics* edited by E Wolf (North-Holland, Amsterdam, 1998) vol. 38; see also references herein
[3] W Chen and D L Mills, *Phys. Rev. Lett.* **58**, 160 (1987)
[4] C M de Sterke and J E Sipe, in *Progress in optics* edited by E Wolf (North-Holland, Amsterdam, 1994) vol. 33
[5] T G Brown and B J Eggleton, *Opt. Exp.* **3**, 385 (1998)
[6] N D Sankhey, D F Prelewitz and T G Brown, *Appl. Phys. Lett.* **60**, 1427 (1992)
N D Sankhey, D F Prelewitz and T G Brown, *J. Appl. Phys.* **73**, 1 (1993)
J He and M Cada, *J. Quantum. Electron.* **27**, 1182 (1991)
[7] B J Eggleton, R E Slusher, C M de Sterke, P A Krug and J E Sipe, *Phys. Rev. Lett.* **76**, 627 (1996)
[8] N G R Broderick, D J Richardson and M Isben, *Opt. Lett.* **25**, 536 (2000)
P Millar, R M De La Rue, T F Krauss, J S Aitchison, N G R Broderick and D J Richardson, *Opt. Lett.* **24**, 685 (1999)
[9] D Taverner, N G R Broderick, D J Richardson, M Isben and R I Laming, *Opt. Lett.* **23**, 259 (1998)
[10] H G Winful and V Perlin, *Phys. Rev. Lett.* **84**, 3586 (2000)
[11] S Dutta Gupta and J Jose, *Opt. Commun.* **125**, 105 (1996)
[12] J Jose and S Dutta Gupta, *Opt. Commun.* **145**, 220 (1998)
[13] T A Laine: Electromagnetic wave propagation in non-linear Kerr media, Doctoral Thesis (Royal Institute of Technology, Stockholm, 2000)
T A Laine and A T Friberg, *Opt. Commun.* **159**, 93 (1998)
T A Laine and A T Friberg, *Appl. Phys. Lett.* **74**, 3248 (1999)
[14] G S Agarwal, *Opt. Commun.* **47**, 77 (1983)
[15] M Born and E Wolf, in *Principles of optics* (Pergamon, New York, 1980) ch. 1
[16] For results pertaining to the linear counterpart, see P Yeh, *J. Opt. Soc. Am.* **A2**, 568 (1985)
[17] S Dutta Gupta, *J. Opt. Soc. Am.* **B6**, 1927 (1989)
[18] A E Kaplan and C T Law, *IEEE J. Quantum. Electron.* **QE-21**, 1529 (1985)